Clinical significance of strain rate stress echocardiography in the early phase of acute myocardial infarction

Wook-Jin Chung

Department of Medicine

The Graduate School, Yonsei University

Clinical significance of strain rate stress echocardiography in the early phase of acute myocardial infarction

Directed by Professor Namsik Chung

Doctoral Dissertation
submitted to the Department of Medicine,
the Graduate School of Yonsei University
in partial fulfillment of the requirements for the degree
of Doctor of Philosophy

Wook-Jin Chung

June 2009

This certifies that the Doctoral Dissertation of Wook-Jin Chung is approved.

Thesis Supervisor : Namsik Chung

Thesis Committee Member : Byung-Chul Chang

Thesis Committee Member : Joong Woo Leem

Thesis Committee Member : Se-Joong Rim

Thesis Committee Member: Jong-Won Ha

The Graduate School
Yonsei University

June 2009

ACKNOWLEDGEMENTS

I would like to express my gratitude to my mentor, Namsik Chung for his considered advice and encouragement that has helped me to accomplish this thesis. Also I appreciated professors, Byung-Chul Chang, Joong Woo Leem, Se-Joong Rim and Jong-Won Ha for providing valuable stimulations and suggestions.

This dissertation is not possible without support and understanding from my families, my wife, Jeong Seon, my sons Yoon-Jae and Yoon-Seong and my parents who believe in me always.

<TABLE OF CONTENTS>

LIST OF FIGURES

LIST OF TABLES

<ABSTRACT>

Clinical significance of strain rate stress echocardiography in the early phase of acute myocardial infarction

Wook-Jin Chung

Department of Medicine

The Graduate School, Yonsei University

(Directed by Professor Namsik Chung)

Background: Strain rate stress echocardiography (SRSE) offers left ventricular (LV) remodeling and even survival data in patients with suspected coronary artery disease. However, there are few reports about the role of SRSE on LV remodeling and survival in patients with acute myocardial infarction (AMI). And, the value of SRI parameters about diastolic and time interval was not fully evaluated in AMI. The aim of this study was to evaluate whether SRSE reflects initial LV diastolic function and predicts late LV remodeling and long-term prognosis by comprehensive SRI analysis in patients of the early phase after an AMI.

Methods: Prospectively, 134 consecutive patients with AMI and akinetic wall motion in at least two segments were enrolled and underwent low-dose dobutamine stress echocardiography (LDDSE) 5~9 days after the event. The peak systolic tissue velocity, peak systolic strain, and seven strain rate parameters, including the peak systolic and diastolic strain rate and each timing parameters were measured at baseline and 10 mcg of the LDDSE. All 9 parameters were transformed to mean (segmental) and sum value of akinetic segments and mean (global) value of all segments. Within 6 hours of the LDDSE, left and right heart catheterization with recording of the LV end diastolic and pulmonary capillary wedge pressures were performed. Follow-up echocardiography with measurement of NT-proBNP was performed after 6 months. At the end of the study, we collected long-term follow-up (50.0 ± 2.0 months) data. Altogether, 45 patients and 520 segments were assessed.

Results: The patients (66.7% males; mean age, 58.6±1.9 years; 66.7% anterior wall, and 71.1% ST-segment elevation) tolerated the LDDSE without significant complications. As expected, global peak strain rate of E (SRE) and time-to-peak (TTP) to peak strain rate of A (SRA) at 10 mcg correlated with the E/E' ratio (r=-0.41 and p=0.02 and r=-0.35 and p=0.02, respectively). Interestingly, global TTP-SRA and segmental TTP-SRE at 10mcg independently predicted LV remodeling (an increase of >20% in left

ventricular end diastolic volume) in 6 months of follow-up (β=-0.02 and p=0.04 and β=-0.04 and p=0.03, respectively). However, neither global nor segmental strain rate parameters predicted long-term survival.

Conclusions: Diastolic time-interval strain rate parameters of LDDSE reflected LV diastolic function and late remodeling in the early phase of an AMI, but could not predict long-term survival in this study. Thus, SRSE may provide useful prognostic information for LV remodeling in patients in the early phase of an AMI.

Key words : myocardial infarction, stress echocardiography, Doppler echocardiography, left ventricular remodeling, prognosis

Clinical significance of strain rate stress echocardiography in the early phase of acute myocardial infarction

Wook-Jin Chung

Department of Medicine

The Graduate School, Yonsei University

(Directed by Professor Namsik Chung)

I. INTRODUCTION

Strain rate imaging (SRI) is a recently introduced echocardiographic modality that allows quantitative assessment of segmental myocardial contractility.[1-4] Furthermore, segmental analysis of the peak systolic strain rate (psSR) and the incremental values of the strain rate on dobutamine stress echocardiography (DSE) can detect myocardial viability.[2]

Several experimental and clinical studies have demonstrated that myocardial viability may influence the diastolic function of the left ventricle (LV), which reflects chamber remodeling in the early phase after acute myocardial

infarction (AMI).[5-7] And, two recent clinical studies have demonstrated that segmental analysis of the psSR on strain rate stress echocardiography (SRSE) may offer survival data that is independent and incremental to the standard wall motion score index in patients with suspected coronary artery disease.[8, 9]

However, there are few reports about the role of SRSE on LV remodeling and survival in the early phase after an AMI. And, the value of SRI parameters about diastolic and time-interval was not fully evaluated in AMI. The aim of this study was to evaluate whether SRSE reflects initial LV diastolic function and predicts late LV remodeling and long-term prognosis by comprehensive SRI analysis in patients of the early phase after an AMI.

II. MATERIALS AND METHODS

1. Study population

Between April 2003 and March 2005, 134 consecutive AMI patients with akinetic wall motion on at least two segments by baseline echocardiography were enrolled. Patients who were in hemodynamically unstable state, had an apical infarct, and who had a poor echo window were excluded. We obtained informed consent from all patients. All patients underwent low-dose DSE (LDDSE; up to 10μg/kg/min of dobutamine infusion) with acquisition of tissue Doppler imaging (TDI) and SRI on the 5th to 9th days after the event when it was reported that LV diastolic function was stabilized after the AMI. At the same time, NT-proBNP was measured. Within 6 hrs of the study, left and right heart catheterization for recording of the LV end diastolic pressure (LVEDP) and pulmonary capillary wedge pressure (PCWP) were performed. Six months later, follow-up echocardiography with measurement of NT-proBNP was performed. Sixty-one patients were excluded because of withdrawn consent (n=6), no revascularization procedure (n=38), and loss to follow-up (n=17). At the end of the study, we collected long-term follow-up (50.0 ± 2.0 months) data by review of outpatient clinic records and telephone interviews. In the analysis of digital echocardiographic imaging, 28 patients

were excluded because of incomplete acquisition, and archiving or technical problems, including low frame rate or poor image quality. Finally, 45 patients (58.6 ± 1.9 years, 67% males) and 520 segments were assessed. (Figure 1, Table 1).

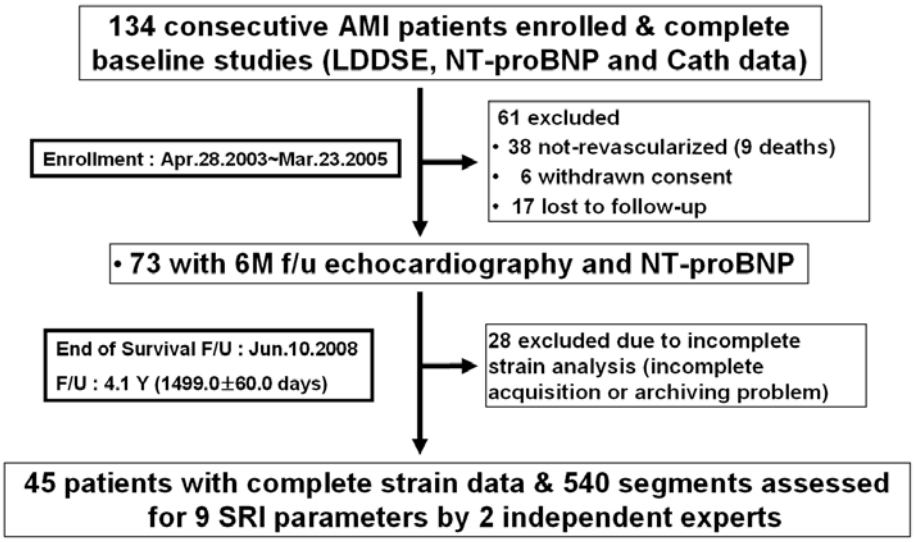

Figure 1. Flow diagram of the study. Altogether, 540 segments from 45 patients were analyzed because apical segments were excluded. AMI; anterior myocardial infarction, LDDSE; low-dose dobutamine stress echocardiography, NT-proBNP; N-terminal pro B-type natriuretic peptide, SRI; strain rate imaging

Table 1. Baseline characteristics of the study population

Variables	**N=45**
Age	58.6±1.9
Gender (M:F)	30:15
Risk Factors	
Current smoking	19 (42.2)
Diabetes	11 (24.4)
Hypertension	14 (31.1)
Medications	
Beta adrenergic blockers	14 (31.1)
ACE* inhibitors or ARBs†	36 (80.0)
STEMI‡ : Non-STEMI	32:13
Location (Anterior / Inferior/ Lateral)	30 /6 /3
Left ventricular ejection fraction (%)	47.7±1.5
LVEDP (mmHg)§	22.3±1.2

Values are expressed as the means ±SEM or n (%).

* ; ACE, angiotensin converting enzyme

† ; ARB, angiotensin II type 1 receptor blocker

‡ ; STEMI, ST segment elevation myocardial infarction

§ : LVEDP, left ventricular end diastolic pressure

2. Low dose dobutamine stress echocardiography

A standard LDDSE protocol was adopted, starting at an infusion rate of 5 μg/kg/min and increasing to 10 μg/kg/min. The duration of each stage was 5 minutes and the blood pressure and imaging were recorded at baseline and the 5th minute of each stage. Images were interpreted off-line by the consensus of two observers using the same 16-segment model. On the basis of subjective visual impressions of the inward motion of the endocardium and thickening of the myocardium, a 5-level scoring system was used for each segment (1=normal, 2=hypokinesia, 3=akinesia, 4=dyskinesia, and 5=aneurysm) and a global LV wall motion score index (WMSI) was computed as the sum of the scores of each segment divided by the number of LV segments.

3. Tissue Doppler imaging and strain rate imaging

TDI and SRI were obtained with a 3.5-MHz transducer in the left lateral decubitus position using a commercially available system (Vivid 7; GE Vingmed, Horten, Norway). TDI and SRI were performed from apical 4-chamber, apical 2-chamber, and apical long-axis views during gray-scale image acquisition at rest and at each stage of LDDSE using a narrow sector angle and high frame rates ($\geq$120 frame/s). This technique uses color tissue

Doppler velocity measurements in each pixel of a sample line to determine spatial velocity gradients along the ultrasound beam according to the equation $SR=[v(r)-v(r+\Delta r)]/\Delta r$, as described previously.[10] The distance along the ultrasound beam is denoted "r" and tissue velocity is denoted "v". Images were obtained at each stage, taking care to align the ventricular walls with the ultrasound beam and to obtain the image during the breath-hold if possible. At least three cardiac cycles were captured and stored digitally. Digital storage of cardiac cycles triggered to the QRS complex was saved for off-line analysis.

4. Strain rate imaging analysis

Analysis was performed offline with dedicated software (Echo-Pac 7.X.X; GE Medical Systems). Measurements were made in each segment of the same model used for WMSI. The region of interest (12x6 mm) was tracked manually and maintained in a fixed mid-myocardial position to make sure the TDI and SRI traces represented the same myocardial segment for the whole cardiac cycle.

The peak systolic tissue velocity (S'), peak systolic strain (psS), and 7 strain rate parameters were measured at baseline and at the peak (10 μg/kg/min) of the LDDSE in 520 segments (12 segments except apical segments for each patient). The strain rate parameters used in this study are summarized in

Figure 2. The psSR was determined as the maximal negative strain rate within 350ms after the R wave, and the peak strain rate of E (SRE) and A (SRA) were also documented.[4] The following 4 time-interval parameters were measured: (1) time-to-peak (TTP) to psSR, (2) time to the onset of regional relaxation (Tr), measured as the difference in time from the R wave to the zero crossover of the strain rate curve at the end of systole,[11] (3) time-to-peak to SRE, and (4) TTP to SRA.

All 9 parameters of TDI and SRI measurements were transformed to mean of akinetic segments (segmental value), sum of akinetic segments (sum of segmental value) and mean of all segments (global value) to compare with the LV remodeling, LV reverse remodeling, myocardial viability and long-term prognosis.

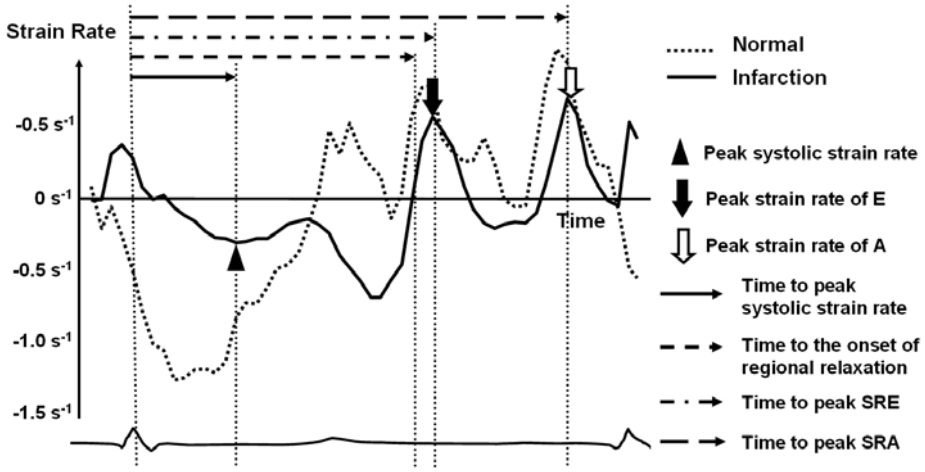

Figure 2. Diagram of strain rate imaging parameters. Cine compound of successive three cycles, moving tracking and angle correction were performed to obtain more objective data and to decrease signal noise.

5. Left and right heart catheterization

All patients underwent left and right heart catheterization via the femoral percutaneous approach with the use of a 6F catheter within 6 hours of the LDDSE. The intracardiac pressure curves of the LVEDP and PCWP were recorded with pigtail catheters before angiography. Measurements were made over 1 respiratory cycle and averaged.

6. Revascularization and follow-up

All patients underwent coronary angiography and subsequent revascularization after LDDSE. The choice of percutaneous or surgical revascularization was based on clinical judgment by the treating physician. Follow-up echocardiography was performed 6 months after revascularization. At the end of the study, long-term follow-up was performed by review of outpatient clinic records and telephone interview with the patient or relative. Cardiac mortality was the primary end point. Patients were censored at the time of percutaneous or surgical revascularization.

LV remodeling was defined as an increase of >20% in LV end diastolic volume (LVEDV) at 6 months from baseline.[12-14] A response of LV reverse-remodeling was defined as a reduction in LV end-systolic volume

(LVESV) of ≥15%.[15-17] Myocardial viability for akinetic segments at baseline was determined by improvement of wall motion at 6 months follow-up echocardiography.

7. Inter- and intra-observer reproducibility

Interobserver variation was assessed by random selection of 10 patients and measurement of SRI by two independent observers using identical images from the same loop of the cardiac cycle. The same 10 patients were chosen for intra-observer variability, in which a single blinded observer repeated the measurements after an interval of 7 days.

8. Statistical analysis

Data were expressed as the mean ± SEM. For comparison of parametric variables between baseline and the 6 month follow-up, the paired sample test with Scheffe's correction was used. To determine for the relationship between wall motion, TDI and SRI variables and initial LV diastolic function, the Spearman's rho test was used.

The Mann-Whitney test was used to detect significant variables influencing on LV remodeling, LV reverse-remodeling and viability. For the univariable

and multivariable analysis of LV remodeling, LV reverse-remodeling and myocardial viability, binary logistic regression was used. In the multivariable analysis, wall motion, TDI and SRI variables were run separately with clinical variables including age, body surface area and diabetes mellitus. To determine for the relationship between TDI and SRI variables and the change of LVEDV and LVESV, the Spearman's rho test was used.

The Cox proportional hazards was used to identify predictors of survival. The cut points for SRI variables were assessed from the derivation sample by initially using a receiver-operating curve analysis. Kaplan-Meier curves were used to estimate the survival function for time-to-death, and a log-rank test was used to compare differences between survival curves. The log-rank test was used to test for significant differences in survival.

The $p < 0.05$ was considered statistically significant. Statistical analysis was conducted using SPSS, version 15.0 (SPSS Inc., Chicago, IL, USA).

III. RESULTS

1. Changes of parameters during follow-up

Changes in the echocardiographic parameters and NT-proBNP levels during the 6 month follow-up are summarized in Table 2. The LV systolic and diastolic parameters and NT-proBNP levels were significantly improved.

Table 2. Changes of echocardiographic parameters and NT-proBNP between baseline and 6 month follow-up

	Baseline	6 month F/U	*p*
LVEF* (%)	47.7±1.5	52.0±1.1	0.000
LVEDV† (mmHg)	94.0±4.0	89.1±3.8	0.000
LVESV‡ (mmHg)	48.8±3.1	44.7±3.1	0.000
E/A ratio	1.3±0.1	1.0±0.1	0.000
EDT§ (msec)	170.6±6.1	200.7±5.9	0.006
E/E' ratio	16.2±1.1	13.2±0.7	0.003
A-a duration ‖ (msec)	24.2±7.1	-10.6±5.8	0.001
LAVI¶ (cc/m2)	30.2±1.1	27.6±1.2	0.000
NT-proBNP** (pg/ml)	1536.9±247.8	347.6±68.7	0.000

Values are expressed as the means ±SEM.

* ; left ventricular ejection fraction

† ; left ventricular end diastolic volume

‡ ; left ventricular end systolic volume

§ ; deceleration time of E wave

|| ; transmitral A – pulmonary venous flow atrial flow reversal duration difference

¶ ; left atrial volume index

**; N-terminal pro B-type natriuretic peptide

2. Variables influencing LV diastolic parameters

Global strain parameters, SRE and TTP-SRA at 10mcg had significant correlations with the E/E' ratio (r=-0.41 and *p*=0.02 and r=-0.35 and *p*=0.02, respectively; Table 3). And also global psS at 10mcg, incremental value of global psS and global S' at 10 mcg was significantly correlated with the E/E' ratio (r=-0.55, *p*=0.00, r=-0.47, *p*=0.00 and r=-0.53, *p*=0.00, respectively; Table 3).

Sum of segmental TTP-SRE at 10mcg and segmental psS showed statistically significant correlations with LVEDP (r=0.35 and *p*=0.02 and r=0.49 and *p*=0.00, respectively).

Table 3. Correlations with wall motion, TDI and SRI variables with E/E' ratio

	r	*P*
G-SRE* at peak (s^{-1})	-0.414	0.02
G-TTP-SRA† at peak (msec)	-0.350	0.02
G-psS‡ at peak	0.547	0.00
Δ G-psS	-0.472	0.00
G-S'§ at peak (cm/s)	-0.525	0.00
WMSI ‖ at peak	0.565	0.00

* ; global peak strain rate of E

† ; global time-to-peak to peak strain rate of A

‡ ; global peak systolic strain

§ ; global peak systolic tissue velocity

‖ ; wall motion score index

3. Variables predicting LV remodeling

Table 4, 5 and 6 showed global, segmental and sum of segmental SRI and TDI values according to the presence of LV remodeling which was defined an increase of >20% in LVEDV.

In global values, TTP-psSR at baseline, TTP-SRE at 10mcg, TTP-SRA at 10mcg and the incremental value of TTP-SRA showed significant differences according to LV remodeling (p=0.02, p=0.01, p=0.01 and p=0.04, respectively; Table 4). Segmental TTP-SRE at 10mcg, segmental TTP-SRA at 10mcg and the incremental value of segmental TTP-SRA also reflect LV remodeling (p=0.01, p=0.00 and p=0.03, respectively; Table 5). Furthermore, the incremental value of sum of segmental TTP-SRA had significance in late LV remodeling (p=0.02; Table 6).

Interestingly, global TTP-SRA at 10mcg and segmental TTP-SRE at 10mcg independently predicts LV remodeling in 6 months of follow-up (β=-0.02 and p=0.04 and β=-0.04 and p=0.03, respectively; Table 7). Also, these two parameters significantly correlated with change of LVEDV (r=-0.40 and p=0.02 and r=-0.41 and p=0.02, respectively; Figure 3).

Table 4. Global SRI, TDI and wall motion variables predicting LV remodeling

	No Remodeling (n=25)	Remodeling (n=7)	*P*
G-psSR* baseline (s^{-1})	-0.76±0.05	-0.86±0.10	0.598
G-psSR at peak (s^{-1})	-1.06±0.09	-1.01±0.21	0.777
Δ G-psSR (s^{-1})	-0.30±0.12	-0.15±0.24	0.884
G-SRE† baseline (s^{-1})	0.93±0.04	0.84±0.13	0.359
G-SRE at peak (s^{-1})	1.16±0.05	0.99±0.15	0.206
Δ G-SRE baseline (s^{-1})	0.22±0.06	0.15±0.03	0.485
G-SRA‡ baseline (s^{-1})	0.95±0.07	0.92±0.28	0.760
G-SRA at peak (s^{-1})	1.09±0.08	1.13±0.17	0.694
Δ G-SRA baseline (s^{-1})	0.14±0.04	0.21±0.13	0.513
G-TTP-psSR§ baseline (msec)	141.47±4.78	131.30±1.88	0.020
G-TTP-psSR at peak (msec)	187.62±63.58	111.87±12.32	0.282
Δ G-TTP-psSR (msec)	59.74±87.93	-19.42±11.88	0.884
G-Tr ‖ at baseline (msec)	313.20±5.05	292.84±7.79	0.079
G-Tr at peak (msec)	261.75±7.40	240.41±8.08	0.116
Δ G-Tr (msec)	-51.44±6.39	-52.44±11.96	0.873
G-TTP-SRE¶ baseline (msec)	505.32±9.92	484.70±16.78	0.264
G-TTP-SRE at peak (msec)	444.95±8.55	394.32±15.29	0.011
Δ G-TTP-SRE (msec)	-60.37±14.51	-90.38±19.21	0.305

G-TTP-SRA** baseline (msec)	788.41±22.57	725.25±41.04	0.194
G-TTP-SRA at peak (msec)	724.31±27.63	575.54±28.91	0.007
Δ G-TTP-SRA (msec)	-64.11±18.61	-149.71±31.10	0.043
G-psS†† baseline	-0.79±0.04	-0.66±0.16	0.614
G-psS at peak	-0.98±0.11	-0.91±0.23	0.538
Δ G-psS	-0.19±0.09	-0.24±0.09	0.695
G-S' ‡‡ baseline (cm/s)	3.58±0.15	2.76±0.71	0.370
G-S' at peak (cm/s)	5.25±0.34	4.34±1.10	0.654
Δ G-S' (cm/s)	1.67±0.24	1.58±0.50	0.780
WMSI§§ baseline	1.70±0.06	1.81±0.13	0.293
WMSI at peak	1.58±0.06	1.71±0.16	0.394
Δ WMSI	-0.11±0.03	-0.11±0.05	0.980

Values are expressed as the means ±SEM.

* ; global peak systolic strain rate

† ; global peak strain rate of E

‡ ; global peak strain rate of A

§ ; global time-to-peak to peak systolic strain rate

‖ ; global time to the onset of regional relaxation

¶ ; global time-to-peak to peak strain rate of E

**; global time-to-peak to peak strain rate of A

††; global peak systolic strain

‡‡; global peak systolic tissue velocity

§§; wall motion score index

Table 5. Segmental SRI and TDI variables predicting LV remodeling

	No Remodeling (n=25)	Remodeling (n=7)	*P*
S-psSR* baseline (s^{-1})	-0.59±0.09	-0.46±0.17	0.673
S-psSR at peak (s^{-1})	-0.90±0.15	-0.64±0.33	0.888
Δ S-psSR (s^{-1})	-0.31±0.13	-0.19±0.16	1.000
S-SRE† baseline (s^{-1})	0.94±0.14	0.99±0.16	0.437
S-SRE at peak (s^{-1})	1.07±0.13	1.25±0.32	0.315
Δ S-SRE baseline (s^{-1})	0.13±0.13	0.27±0.35	0.855
S-SRA‡ baseline (s^{-1})	0.92±0.11	0.88±0.10	0.927
S-SRA at peak (s^{-1})	1.12±0.14	1.27±0.21	0.584
Δ S-SRA baseline (s^{-1})	0.20±0.09	0.39±0.13	0.411
S-TTP-psSR§ baseline (msec)	142.32±10.52	125.61±15.12	0.667
S-TTP-psSR at peak (msec)	112.49±10.60	110.61±19.83	0.784
Δ S-TTP-psSR (msec)	-29.82±10.56	-14.99±21.41	0.505
S-Tr ‖ at baseline (msec)	321.97±6.82	306.26±9.97	0.202
S-Tr at peak (msec)	268.82±11.21	246.50±10.11	0.202
Δ S-Tr (msec)	-53.15±10.60	-59.76±14.09	0.777
S-TTP-SRE¶ baseline (msec)	503.88±11.78	476.89±19.51	0.299
S-TTP-SRE at peak (msec)	441.88±8.91	382.97±11.30	0.005
Δ S-TTP-SRE (msec)	-62.01±12.94	-93.92±17.07	0.257

S-TTP-SRA** baseline (msec)	788.71±24.06	718.45±36.65	0.156
S-TTP-SRA at peak (msec)	732.32±27.73	563.32±28.97	0.002
Δ S-TTP-SRA (msec)	-56.40±24.86	-155.13±25.03	0.033
S-psS†† baseline	-0.52±0.06	-0.78±0.14	0.120
S-psS at peak	-0.80±0.07	-1.11±0.15	0.062
Δ S-psS	-0.28±0.06	-0.32±0.14	0.517
S-S' ‡‡ baseline (cm/s)	2.93±0.27	2.83±0.77	0.836
S-S' at peak (cm/s)	4.67±0.44	4.59±1.28	0.717
Δ S-S' (cm/s)	1.74±0.36	1.77±0.65	0.917

Values are expressed as the means ±SEM.

* ; segmental peak systolic strain rate

† ; segmental peak strain rate of E

‡ ; segmental peak strain rate of A

§ ; segmental time-to-peak to peak systolic strain rate

‖ ; segmental time to the onset of regional relaxation

¶ ; segmental time-to-peak to peak strain rate of E

**; segmental time-to-peak to peak strain rate of A

††; segmental peak systolic strain

‡‡; segmental peak systolic tissue velocity

Table 6. Sum of segmental SRI and TDI variables predicting LV remodeling

	No Remodeling (n=25)	Remodeling (n=7)	*P*
Sum-psSR* baseline (s^{-1})	-0.94±0.15	-1.20±0.06	0.232
Sum-psSR at peak (s^{-1})	-1.52±0.30	-1.60±0.35	0.574
Δ Sum-psSR (s^{-1})	-0.58±0.23	-0.40±0.29	0.888
Sum-SRE† baseline (s^{-1})	1.73±0.20	2.59±0.64	0.201
Sum-SRE at peak (s^{-1})	2.10±0.32	2.92±0.24	0.068
Δ Sum-SRE (s^{-1})	0.36±0.23	0.32±0.88	0.927
Sum-SRA‡ baseline (s^{-1})	1.77±0.25	2.38±0.70	0.411
Sum-SRA at peak (s^{-1})	2.17±0.31	3.58±1.37	0.235
Δ Sum-SRA (s^{-1})	0.40±0.22	1.21±0.66	0.273
Sum-TTP-psSR§ baseline (msec)	257.33±40.39	361.76±114.42	0.557
Sum-TTP-psSR at peak (msec)	209.83±35.84	306.37±95.86	0.411
Δ Sum-TTP-psSR (msec)	-47.50±19.29	-55.38±56.48	0.969
Sum-Tr ‖ at baseline (msec)	777.21±97.43	740.85±131.27	0.925
Sum-Tr at peak (msec)	654.05±88.32	618.00±133.76	0.925
Δ Sum-Tr (msec)	-123.16±28.65	-122.86±24.62	0.637
Sum-TTP-SRE¶ baseline (msec)	1224.82±160.54	1181.12±242.13	0.887
Sum-TTP-SRE at peak (msec)	1058.21±133.40	944.34±185.37	0.777

Δ Sum-TTP-SRE (msec)	-166.61±46.39	-236.78±79.96	0.143
Sum-TTP-SRA** baseline (msec)	1870.57±236.66	1753.89±319.91	0.962
Sum-TTP-SRA peak (msec)	1703.37±205.29	1360.90±229.31	0.603
Δ Sum-TTP-SRA (msec)	-167.20±67.70	-392.99±115.69	0.018
Sum-psS†† baseline	-1.14±0.17	-1.39±0.23	0.324
Sum-psS at peak	-1.71±0.20	-2.20±0.30	0.108
Δ Sum-psS	-0.57±0.12	-0.82±0.13	0.139
Sum-S' ‡‡ baseline	7.37±1.22	5.84±1.65	0.756
Sum-S' at peak	11.73±1.88	9.48±2.54	0.717
Δ Sum-S'	4.36±0.90	3.64±1.25	0.795

Values are expressed as the means ±SEM.

* ; sum of segmental peak systolic strain rate

† ; sum of segmental peak strain rate of E

‡ ; sum of segmental peak strain rate of A

§ ; sum of segmental time-to-peak to peak systolic strain rate

‖ ; sum of segmental time to the onset of regional relaxation

¶ ; sum of segmental time-to-peak to peak strain rate of E

**; sum of segmental time-to-peak to peak strain rate of A

††; sum of segmental peak systolic strain

‡‡; sum of segmental peak systolic tissue velocity

Table 7. Prediction of LV remodeling by univariable and multivariable analysis of SRSE variables

	Univariable Analysis		Multivariable Analysis	
	β	*p*	β	*p*
G-TTP-psSR* baseline (msec)	-0.054	0.228	-0.031	0.496
G-TTP-SRE† at peak (msec)	-0.031	0.025	-0.029	0.062
G-TTP-SRA‡ at peak (msec)	-0.016	0.020	-0.019	0.039
Δ G-TTP-SRA (msec)	-0.010	0.050	-0.010	0.091
S-TTP-SRE§ at peak (msec)	-0.039	0.014	-0.043	0.033
S-TTP-SRA ‖ at peak (msec)	-0.018	0.011	-0.109	0.170
Δ S-TTP-SRA (msec)	-0.009	0.062	-0.009	0.105
Δ Sum-TTP-SRA¶ (msec)	-0.002	0.140	-0.002	0.176

For the multivariable analysis, wall motion, TDI and SRI variables were run separately with clinical variables including age, body surface area and diabetes mellitus.

* ; global time-to-peak to peak systolic strain rate

† ; global time-to-peak to peak strain rate of E

‡ ; global time-to-peak to peak strain rate of A

§ ; segmental time-to-peak to peak strain rate of E

‖ ; segmental time-to-peak to peak strain rate of A

¶ ; sum of segmental time-to-peak to peak strain rate of A

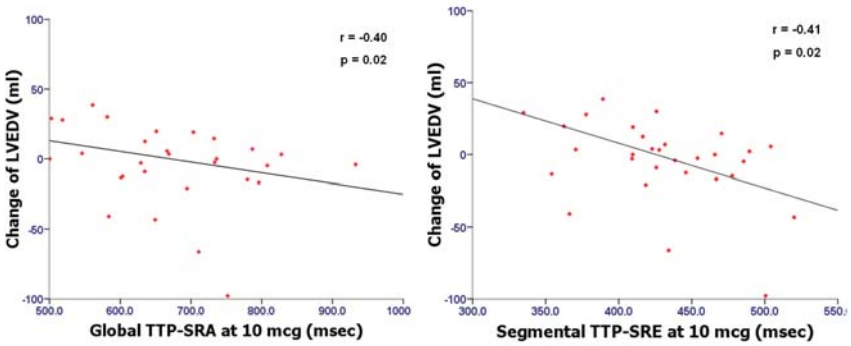

Figure 3. Correlations between global time-to-peak strain rate of A (left) and segmental time-to-peak strain rate of E (right) at 10 mcg of low-dose dobutamine stress echocardiography with the change of left ventricular end diastolic volume (LVEDV).

4. Variables predicting LV reverse-remodeling

Table 8, 9 and 10 showed global, segmental and sum of segmental SRI and TDI values according to the presence of LV reverse-remodeling which was defined as a reduction in LV end-systolic volume of ≥15%.

The incremental value of segmental TTP-psSR reflect LV reverse-remodeling (p=0.04; Table 9). However, it could not show statistical significance predicting LV reverse-remodeling in logistic regression (Table 11).

Table 8. Global SRI, TDI and wall motion variables predicting LV reverse-remodeling

	No Reverse-Remodeling (n=21)	Reverse-Remodeling (n=10)	*P*
G-psSR* baseline (s^{-1})	-0.78±0.05	-0.80±0.11	0.628
G-psSR at peak (s^{-1})	-1.14±0.14	-0.90±0.05	0.077
Δ G-psSR (s^{-1})	-0.36±0.16	-0.11±0.16	0.116
G-SRE† baseline (s^{-1})	0.90±0.06	0.96±0.07	0.495
G-SRE at peak (s^{-1})	1.15±0.07	1.15±0.08	0.804
Δ G-SRE baseline (s^{-1})	0.25±0.05	0.19±0.11	0.457
G-SRA‡ baseline (s^{-1})	0.92±0.10	0.97±0.12	0.438
G-SRA at peak (s^{-1})	1.06±0.10	1.13±0.12	0.577
Δ G-SRA baseline (s^{-1})	0.15±0.06	0.16±0.06	0.951
G-TTP-psSR§ baseline (msec)	138.79±2.24	138.99±15.16	0.544
G-TTP-psSR at peak (msec)	191.13±78.99	133.91±8.27	0.239
Δ G-TTP-psSR (msec)	54.36±77.82	-5.09±10.72	0.644
G-Tr ‖ at baseline (msec)	306.29±5.63	312.11±8.35	0.767
G-Tr at peak (msec)	250.75±7.25	272.95±11.57	0.108
Δ G-Tr (msec)	-55.54±6.69	-39.16±9.40	0.190

G-TTP-SRE¶ baseline (msec)	507.69±11.54	490.89±12.11	0.398
G-TTP-SRE at peak (msec)	426.45±10.53	453.37±12.77	0.118
Δ G-TTP-SRE (msec)	-81.24±15.88	-37.51±17.60	0.091
G-TTP-SRA** baseline (msec)	760.57±24.87	806.25±37.08	0.353
G-TTP-SRA at peak (msec)	681.74±32.82	721.65±39.86	0.398
Δ G-TTP-SRA (msec)	-78.83±22.52	-84.60±28.05	0.933
G-psS†† baseline	-0.73±0.06	-0.84±0.07	0.411
G-psS at peak	-0.91±0.14	-1.06±0.09	0.918
Δ G-psS	-0.18±0.11	-0.22±0.08	0.797
G-S' ‡‡ baseline (cm/s)	3.32±0.28	3.49±.024	0.959
G-S' at peak (cm/s)	4.86±0.47	5.30±0.57	0.719
Δ G-S' (cm/s)	1.53±0.26	1.81±0.42	0.537
WMSI§§ baseline	1.76±0.05	1.65±0.15	0.234
WMSI at peak	1.65±0.07	1.54±0.11	0.440
Δ WMSI	-0.11±0.02	-0.11±0.06	0.637

Values are expressed as the means ±SEM.

* ; global peak systolic strain rate

† ; global peak strain rate of E

‡ ; global peak strain rate of A

§ ; global time-to-peak to peak systolic strain rate

|| ; global time to the onset of regional relaxation

¶ ; global time-to-peak to peak strain rate of E

**; global time-to-peak to peak strain rate of A

††; global peak systolic strain

‡‡; global peak systolic tissue velocity

§§; wall motion score index

Table 9. Segmental SRI and TDI variables predicting LV reverse-remodeling

	No Reverse-Remodeling (n=21)	Reverse-Remodeling (n=10)	*P*
S-psSR* baseline (s^{-1})	-0.57±0.10	-0.59±0.14	0.892
S-psSR at peak (s^{-1})	-0.97±0.21	-0.71±0.10	0.683
Δ S-psSR (s^{-1})	-0.40±0.15	-0.12±0.15	0.441
S-SRE† baseline (s^{-1})	0.99±0.15	0.93±0.23	0.216
S-SRE at peak (s^{-1})	1.14±0.19	1.10±0.14	0.764
Δ S-SRE baseline (s^{-1})	0.15±0.17	0.17±0.20	0.973
S-SRA‡ baseline (s^{-1})	0.98±0.13	0.80±0.15	0.504
S-SRA at peak (s^{-1})	1.18±0.19	1.10±0.16	0.894
Δ S-SRA baseline (s^{-1})	0.20±0.13	0.30±0.10	0.867
S-TTP-psSR§ baseline (msec)	125.53±7.02	163.81±21.78	0.101
S-TTP-psSR at peak (msec)	112.87±9.93	112.53±21.99	1.000
Δ S-TTP-psSR (msec)	-12.66±10.02	-51.29±18.71	0.037
S-Tr ‖ at baseline (msec)	318.65±6.07	316.25±14.63	0.541
S-Tr at peak (msec)	253.77±11.01	290.79±14.78	0.081
Δ S-Tr (msec)	-64.88±9.87	-25.45±15.61	0.099

S-TTP-SRE¶ baseline (msec)	496.59±11.97	497.29±22.16	0.946
S-TTP-SRE at peak (msec)	422.68±9.76	440.41±18.90	0.378
Δ S-TTP-SRE (msec)	-73.91±12.57	-56.88±24.10	0.354
S-TTP-SRA** baseline (msec)	764.19±27.09	792.89±35.25	0.483
S-TTP-SRA at peak (msec)	693.86±36.34	705.13±26.34	0.603
Δ S-TTP-SRA (msec)	-70.32±27.11	-87.76±37.38	0.946
S-psS†† baseline	-0.58±0.08	-0.55±0.06	0.869
S-psS at peak	-0.83±0.09	-0.91±0.07	0.423
Δ S-psS	-0.25±0.07	-0.36±0.09	0.437
S-S' ‡‡ baseline (cm/s)	2.92±0.32	2.82±0.52	1.000
S-S' at peak (cm/s)	4.64±0.50	4.24±0.79	0.777
Δ S-S' (cm/s)	1.72±0.37	1.43±0.55	0.671

Values are expressed as the means ±SEM.

* ; segmental peak systolic strain rate

† ; segmental peak strain rate of E

‡ ; segmental peak strain rate of A

§ ; segmental time-to-peak to peak systolic strain rate

|| ; segmental time to the onset of regional relaxation

¶ ; segmental time-to-peak to peak strain rate of E

**; segmental time-to-peak to peak strain rate of A

††; segmental peak systolic strain

‡‡; segmental peak systolic tissue velocity

Table 10. Sum of segmental SRI and TDI variables predicting LV reverse-remodeling

	No Reverse-Remodeling (n=21)	Reverse-Remodeling (n=10)	*P*
Sum-psSR* baseline (s^{-1})	-0.91±0.10	-1.05±0.32	0.618
Sum-psSR at peak (s^{-1})	-1.54±0.26	-1.51±0.59	0.389
Δ Sum-psSR (s^{-1})	-0.62±0.25	-0.46±0.37	0.469
Sum-SRE† baseline (s^{-1})	1.93±0.25	1.81±0.37	0.640
Sum-SRE at peak (s^{-1})	2.20±0.26	2.36±0.64	0.570
Δ Sum-SRE (s^{-1})	0.27±0.24	0.55±0.44	0.920
Sum-SRA‡ baseline (s^{-1})	2.05±0.36	1.53±0.28	0.423
Sum-SRA at peak (s^{-1})	2.43±0.49	2.30±0.48	0.947
Δ Sum-SRA (s^{-1})	0.39±0.29	0.77±0.33	0.815
Sum-TTP-psSR§ baseline (msec)	273.17±51.21	296.08±79.87	0.881
Sum-TTP-psSR at peak (msec)	248.71±47.21	203.14±60.27	0.765
Δ Sum-TTP-psSR (msec)	-24.46±24.01	-92.94±29.51	0.086
Sum-Tr ‖ at baseline (msec)	780.50±79.50	753.56±214.11	0.402
Sum-Tr at peak (msec)	639.34±75.40	681.67±191.15	0.839
Δ Sum-Tr (msec)	-141.17±24.61	-71.89±50.97	0.108

Sum-TTP-SRE¶ baseline (msec)	1228.27±134.82	1201.66±354.25	0.378
Sum-TTP-SRE at peak (msec)	1033.44±104.94	1045.95±304.82	0.572
Δ Sum-TTP-SRE (msec)	-194.83±47.74	-155.71±84.62	0.213
Sum-TTP-SRA** baseline (msec)	1837.61±186.07	1892.49±535.39	0.455
Sum-TTP-SRA peak (msec)	1643.11±166.14	1633.20±446.11	0.378
Δ Sum-TTP-SRA (msec)	-194.50±67.67	-259.29±139.54	0.910
Sum-psS†† baseline	-1.16±0.17	-1.25±0.32	0.981
Sum-psS at peak	-1.76±0.18	-1.91±0.44	0.671
Δ Sum-psS	-0.60±0.12	-0.66±0.22	0.777
Sum-S' ‡‡ baseline	6.99±1.07	7.22±2.58	0.637
Sum-S' at peak	10.81±1.58	11.65±4.04	0.637
Δ Sum-S'	3.82±0.81	4.42±1.72	0.925

Values are expressed as the means ±SEM.

* ; sum of segmental peak systolic strain rate

† ; sum of segmental peak strain rate of E

‡ ; sum of segmental peak strain rate of A

§ ; sum of segmental time-to-peak to peak systolic strain rate

|| ; sum of segmental time to the onset of regional relaxation

¶ ; sum of segmental time-to-peak to peak strain rate of E

**; sum of segmental time-to-peak to peak strain rate of A

††; sum of segmental peak systolic strain

‡‡; sum of segmental peak systolic tissue velocity

Table 11. Prediction of LV reverse-remodeling by univariable and multivariable analysis of SRSE variables

	Univariable Analysis		Multivariable Analysis	
	β	*p*	β	*p*
Δ S-TTP-psSR* (msec)	-0.025	0.085	-0.022	0.173

For the multivariable analysis, wall motion, TDI and SRI variables were run separately with clinical variables including age, body surface area and diabetes mellitus.

* ; segmental time-to-peak to peak systolic strain rate

5. Variables predicting myocardial viability

Table 12, 13 and 14 showed global, segmental and sum of segmental SRI and TDI values according to the presence of viable myocardium which was determined by the comparison of akinetic segments at initial and 6 month follow up echocardiography.

Segmental S' and Sum of S' at baseline reflect myocardial viability (p=0.04 and p=0.04; Table 12-13). However, Sum of S' only show statistical significance predicting myocardial viability in logistic regression (β=0.17 and p=0.04; Table 15).

The presence of viable myocardium significantly decreased LVEDV. (p=0.01; Figure 4).

Table 12. Global SRI, TDI and wall motion variables predicting myocardial viability

	Non-viable (n=19)	Viable (n=12)	*P*
G-psSR* baseline (s^{-1})	-0.80±0.05	-0.68±0.09	0.313
G-psSR at peak (s^{-1})	-1.08±0.11	-0.91±0.06	0.126
Δ G-psSR (s^{-1})	-0.28±0.13	-0.26±0.01	0.844
G-SRE† baseline (s^{-1})	0.91±0.06	0.86±0.07	0.697
G-SRE at peak (s^{-1})	1.15±0.07	1.06±0.08	0.452
Δ G-SRE baseline (s^{-1})	0.24±0.04	0.19±0.10	0.483
G-SRA‡ baseline (s^{-1})	0.91±0.09	0.88±0.11	0.938
G-SRA at peak (s^{-1})	1.12±0.09	1.04±0.11	0.517
Δ G-SRA baseline (s^{-1})	0.21±0.06	0.16±0.05	0.622
G-TTP-psSR§ baseline (msec)	139.96±5.99	150.75±8.79	0.166
G-TTP-psSR at peak (msec)	181.40±64.15	130.54±9.26	0.462
Δ G-TTP-psSR (msec)	38.09±63.98	-35.43±4.89	0.324
G-Tr ‖ at baseline (msec)	304.16±7.01	308.02±6.67	0.968
G-Tr at peak (msec)	247.90±8.10	261.65±8.99	0.292
Δ G-Tr (msec)	-56.26±7.61	-46.37±7.63	0.311
G-TTP-SRE¶ baseline (msec)	505.49±11.66	494.92±12.10	0.776

G-TTP-SRE at peak (msec)	429.07±11.95	443.33±10.86	0.394
Δ G-TTP-SRE (msec)	-76.42±16.65	-51.59±18.45	0.516
G-TTP-SRA** baseline (msec)	776.29±34.85	765.59±28.81	0.839
G-TTP-SRA at peak (msec)	687.33±36.09	686.14±28.52	0.871
Δ G-TTP-SRA (msec)	-88.97±23.70	-79.45±25.13	0.839
G-psS†† baseline	-0.76±0.05	-0.73±0.07	0.521
G-psS at peak	-1.08±0.05	-0.78±0.20	0.093
Δ G-psS	-0.32±0.03	-0.05±0.18	0.167
G-S' ‡‡ baseline (cm/s)	3.42±0.20	3.83±0.24	0.236
G-S' at peak (cm/s)	5.17±0.40	5.43±0.52	0.730
Δ G-S' (cm/s)	1.75±0.26	1.59±0.37	0.730
WMSI§§ baseline	1.74±0.06	1.82±0.15	1.000
WMSI at peak	1.64±0.07	1.66±0.12	0.984
Δ WMSI	-0.10±0.02	-0.16±0.04	0.266

Values are expressed as the means ±SEM.

* ; global peak systolic strain rate

† ; global peak strain rate of E

‡ ; global peak strain rate of A

§ ; global time-to-peak to peak systolic strain rate

‖ ; global time to the onset of regional relaxation

¶ ; global time-to-peak to peak strain rate of E

**; global time-to-peak to peak strain rate of A

††; global peak systolic strain

‡‡; global peak systolic tissue velocity

§§; wall motion score index

Table 13. Segmental SRI and TDI variables predicting myocardial viability

	Non-viable (n=19)	Viable (n=12)	*P*
S-psSR* baseline (s^{-1})	-0.61±0.08	-0.48±0.14	0.426
S-psSR at peak (s^{-1})	-0.94±0.18	-0.69±0.09	0.664
Δ S-psSR (s^{-1})	-0.32±0.14	-0.20±0.13	0.828
S-SRE† baseline (s^{-1})	0.91±0.14	0.87±0.20	0.516
S-SRE at peak (s^{-1})	1.19±0.19	0.99±0.11	0.622
Δ S-SRE baseline (s^{-1})	0.28±0.17	0.12±0.15	0.392
S-SRA‡ baseline (s^{-1})	0.95±0.12	0.77±0.13	0.406
S-SRA at peak (s^{-1})	1.19±0.16	0.95±0.15	0.452
Δ S-SRA baseline (s^{-1})	0.24±0.10	0.18±0.11	0.516
S-TTP-psSR§ baseline (msec)	132.99±8.72	153.75±21.10	0.540
S-TTP-psSR at peak (msec)	121.35±10.37	115.29±20.97	0.854
Δ S-TTP-psSR (msec)	-11.64±11.36	-38.46±20.14	0.221
S-Tr ‖ at baseline (msec)	307.93±6.21	328.36±10.96	0.123
S-Tr at peak (msec)	249.60±11.75	285.27±13.30	0.068
Δ S-Tr (msec)	-58.33±10.82	-43.09±14.16	0.570
S-TTP-SRE¶ baseline (msec)	502.07±13.97	502.21±20.15	0.903

S-TTP-SRE at peak (msec)	426.46±10.21	440.10±15.10	0.491
Δ S-TTP-SRE (msec)	-75.61±10.84	-62.11±23.88	0.776
S-TTP-SRA** baseline (msec)	784.08±38.45	777.92±32.39	0.839
S-TTP-SRA at peak (msec)	708.53±40.55	690.57±24.80	0.871
Δ S-TTP-SRA (msec)	-75.55±32.55	-87.34±26.01	0.968
S-psS†† baseline	-0.60±0.07	-0.45±0.06	0.096
S-psS at peak	-0.77±0.09	-0.80±0.07	0.715
Δ S-psS	-0.17±0.08	-0.36±0.07	0.128
S-S' ‡‡ baseline (cm/s)	2.63±0.29	3.51±0.40	0.039
S-S' at peak (cm/s)	4.35±0.56	5.00±0.58	0.330
Δ S-S' (cm/s)	1.73±0.43	1.48±0.44	0.903

Values are expressed as the means ±SEM.

* ; segmental peak systolic strain rate

† ; segmental peak strain rate of E

‡ ; segmental peak strain rate of A

§ ; segmental time-to-peak to peak systolic strain rate

|| ; segmental time to the onset of regional relaxation

¶ ; segmental time-to-peak to peak strain rate of E

**; segmental time-to-peak to peak strain rate of A

††; segmental peak systolic strain

‡‡; segmental peak systolic tissue velocity

Table 14. Sum of segmental SRI and TDI variables predicting myocardial viability

	Non-Viable (n=19)	Viable (n=12)	*P*
Sum-psSR* baseline (s^{-1})	-1.02±0.17	-0.97±0.30	0.538
Sum-psSR at peak (s^{-1})	-1.53±0.28	-1.70±0.49	0.885
Δ Sum-psSR (s^{-1})	-0.52±0.22	-0.73±0.37	0.638
Sum-SRE† baseline (s^{-1})	1.60±0.22	1.97±0.31	0.406
Sum-SRE at peak (s^{-1})	2.03±0.24	2.52±0.51	0.659
Δ Sum-SRE (s^{-1})	0.42±0.23	0.56±0.37	0.775
Sum-SRA‡ baseline (s^{-1})	1.75±0.29	1.86±0.31	0.678
Sum-SRA at peak (s^{-1})	2.26±0.42	2.31±0.42	0.659
Δ Sum-SRA (s^{-1})	0.51±0.22	0.45±0.34	0.483
Sum-TTP-psSR§ baseline (msec)	260.83±57.43	323.19±65.59	0.358
Sum-TTP-psSR at peak (msec)	231.17±44.22	254.28±61.10	0.582
Δ Sum-TTP-psSR (msec)	-29.66±23.01	-68.91±37.29	0.126
Sum-Tr ‖ at baseline (msec)	638.13±83.91	941.19±163.65	0.114
Sum-Tr at peak (msec)	534.12±79.47	810.89±147.02	0.068
Δ Sum-Tr (msec)	-104.01±22.65	-130.30±46.15	0.543
Sum-TTP-SRE¶ baseline (msec)	1062.84±154.59	1457.48±272.47	0.194

Sum-TTP-SRE at peak (msec)	886.30±118.73	1264.24±230.34	0.156
Δ Sum-TTP-SRE (msec)	-176.54±44.74	-193.25±84.33	0.839
Sum-TTP-SRA** baseline (msec)	1618.89±247.55	2229.28±407.13	0.224
Sum-TTP-SRA peak (msec)	1420.12±192.20	1975.16±356.97	0.256
Δ Sum-TTP-SRA (msec)	-198.78±84.78	-254.12±104.47	0.656
Sum-psS†† baseline	-1.03±0.13	-1.22±0.26	0.685
Sum-psS at peak	-1.42±0.17	-2.47±0.53	0.114
Δ Sum-psS	-0.39±0.11	-1.26±0.43	0.062
Sum-S' ‡‡ baseline	5.44±0.96	10.57±2.18	0.043
Sum-S' at peak	8.85±1.55	19.69±5.97	0.114
Δ Sum-S'	3.41±0.85	9.12±4.57	0.394

Values are expressed as the means ±SEM.

* ; sum of segmental peak systolic strain rate

† ; sum of segmental peak strain rate of E

‡ ; sum of segmental peak strain rate of A

§ ; sum of segmental time-to-peak to peak systolic strain rate

|| ; sum of segmental time to the onset of regional relaxation

¶ ; sum of segmental time-to-peak to peak strain rate of E

**; sum of segmental time-to-peak to peak strain rate of A

††; sum of segmental peak systolic strain

‡‡; sum of segmental peak systolic tissue velocity

Table 15. Prediction of myocardial viability by univariable and multivariable analysis of SRSE variables

	Univariable Analysis		Multivariable Analysis	
	β	*p*	β	*p*
S-S' * baseline (cm/s)	0.536	0.087	0.697	0.055
Sum-S' † baseline (cm/s)	0.158	0.038	0.174	0.036

For the multivariable analysis, wall motion, TDI and SRI variables were run separately with clinical variables including age, body surface area and diabetes mellitus.

* ; segmental peak systolic tissue velocity

† ; sum of segmental peak systolic tissue velocity

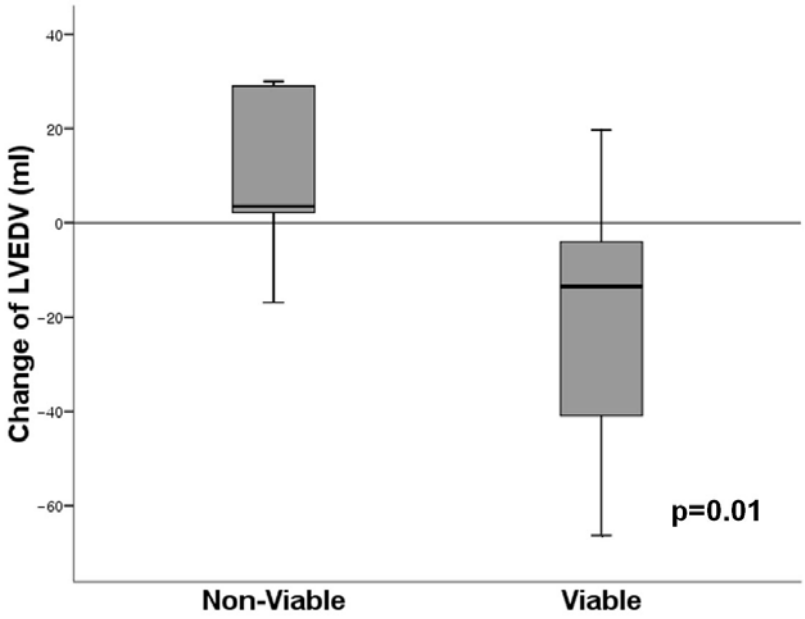

Figure 4. Change of left ventricular end diastolic volume (LVEDV) according to the viability of akinetic myocardial segments.

6. Predictor of cardiovascular mortality

Three patients died during the follow-up period (1499.0 ± 60.0 days). All were cardiovascular mortality. Based on univariable and multivariable analysis, the predictor of death could not be found (Table 16).

Table 16. Prediction of cardiovascular mortality by univariable and multivariable analysis of clinical, echocardiographic, and SRSE variables

	Univariable Analysis		Multivariable Analysis	
	Hazard Ratio (95% CI)	*p*	Hazard Ratio (95% CI)	*p*
Age > 65 years	1.5 (0.1 to 17.0)	0.73	0.05 (0.0 to 2.8)	0.15
Diabetes Mellitus	0.1 (0.01 to 1.2)	0.07	0.2 (0.01 to 2.0)	0.16
LVEF *< 40%	8.4 (0.8 to 92.5)	0.08	18.7 (0.7 to 471.5)	0.08
WMSI† >1.7	4.0 (0.4 to 44.2)	0.26	18.1 (0.4 to 848.1)	0.14
G-TTP-SRA‡ at peak < 707.2 msec	0.4 (0.04 to 4.3)	0.44	0.5 (0.04 to 5.8)	0.58
S-TTP-SRE§ at peak < 433.5 msec	0.4 (0.04 to 4.4)	0.45	0.2 (0.01 to 3.1)	0.17
Sum-S' † baseline < 2.1 cm/s	0.04 (0.0 to 12.1)	0.66	0.0 (0.0 to 63.0)	0.99

* ; left ventricular ejection fraction

† ; wall motion score index

‡ ; global time-to-peak to peak strain rate of A

§ ; segmental time-to-peak to peak strain rate of E

† ; sum of segmental peak systolic tissue velocity

7. Inter- and intra-observer reproducibility

For inter- and intra-observer variation, the correlation coefficients were 0.85 and 0.93, respectively (p=0.00 and p=0.00, respectively).

IV. DISCUSSION

The present study demonstrates for the first time that the role of SRSE on LV remodeling and long-term outcome in the early phase of an AMI. Specifically, two diastolic timing parameters, global TTP-SRA at 10 mcg and segmental TTP-SRE at 10mcg of LDDSE were independent predictors of late LV remodeling in patients with an AMI. We also demonstrated that SRSE reflects LV diastolic parameters and late remodeling by comprehensive stepwise approaches, despite that could not find any predictor in long-term survival data likely because of small number of cardiovascular mortality.

SRI using tissue Doppler data was introduced a decade ago, and has been validated as an objective tool showing myocardial deformation and a predictor for functional recovery and myocardial viability.[1, 2, 10, 18] Because wall motion is known to be subjective and weak in reflecting the severity and extent of ischemic burden, and tissue velocity has significant limitations in evaluating regional function, SRI is expected to determine intrinsic myocardial function. In addition, strain has been reported to be inferior to strain rate data.[19] In the present study, two SRI parameters, global TTP-SRA at 10 mcg and segmental TTP-SRE at 10mcg of LDDSE were independently provide prognostic information for LV remodeling, which was superior than any wall motion, TDI and strain parameters.

Previous studies with myocardial viability and survival mostly reported about systolic strain rate parameters like psSR.[1, 2, 8] An increase of psSR from rest to peak dobutamine stimulation by more than -0.23/s allowed accurate discrimination of viable from nonviable myocardium, as determined by ^{18}F-fluorodeoxyglucose positron emission tomography.[2] Furthermore, psSR of dobutamine stress echocardiography was an independent predictor of all-cause mortality on screening for coronary artery disease.[8] One report about diastolic strain rate in ischemic LV dysfunction showed that SRE and SRA at 20mcg and incremental value of SRE could discriminate myocardial viability. However, in our study, neither systolic nor diastolic value of 'peak' SRI parameters had any statistically significance. It is likely that relatively too low dose dobutamine stimulation to make the significant peak value. Additionally, it seems also that too low dose DSE could not to make a significance of any incremental value of SRSE. In this study, 'diastolic' and 'time-interval' SRI parameters were instead proved the independent predictor of LV remodeling. This is similar to the report about the utility of Tr^{11}. It is postulated that time-interval parameter may be less dependent on the dosage of dobutamine than peak values and also diastolic strain is most likely to link with LV diastolic function and LV remodeling process.

In addition, the present study had other several unique features. Specifically, the present study was prospective rather than a retrospective design, patients

with an AMI rather than suspected coronary artery disease in the study population, and 'low-dose' DSE rather than conventional DSE compared with previous studies about SRSE.[1, 2, 4, 8, 9, 19] Undoubtedly, LDDSE is a safer method in AMI and more favorable in decreasing signal noise than conventional DSE for assessing SRI.[19] Moreover, we took an approach three dataset of SRI, global, segmental and sum of segmental values for the first time. Our original hypothesis was global value was more correlated with intracardiac pressure parameters like noninvasive E/E'ratio and invasive LVEDP and PCWP. As described in Table 3, various global values were significantly correlated to E/E' ratio. However, there were no significant differences among global, segmental and sum of segmental SRI values in predicting LV remodeling. So, further study for the comparison of global and segmental SRI values is needed.

The present study had several limitations. First, because the present study was conducted by Doppler strain, angle dependency, exclusion of apical segments and an only available longitudinal value were expected as weak points. Recently, a 2-dimensinal speckle tracking technique was suggested to be a promising alternative method, especially on DSE, by which a global diastolic strain rate during the isovolumetric relaxation period (SR_{IVR}) was strongly dependent on LV relaxation, and even the E/ SR_{IVR} predicted LV. filling pressures in an animal study.[20-22] Three-dimensional strain analysis

with low-dose dobutamine stimulation was tried in a magnetic resonance imaging field.[23] Unfortunately, two-thirds of patients enrolled were excluded because one-half of them were not revascularized due to insignificant coronary anatomy, which may indicate spontaneous reperfusion after occlusion or spasm. Another comparable number was excluded because of technical problems from incomplete acquisition or archiving problems. As mentioned before, SRI using tissue Doppler need sophisticated techniques to ensure optimizing signal quality and reduction in signal noise, especially at peak stress.[1] Finally, the assessment of SRI is still tremendously time-consuming. So, several automated quantitative techniques are needed to overcome such shortcomings.[8, 9] Recent study reported that an anatomic M-mode technique using psSR independently predicted cardiac events in patients with known or suspected coronary artery disease.[9]

V. CONCLUSION

Diastolic time-interval strain rate parameters of LDDSE reflect LV diastolic function and late remodeling in the early phase of an AMI, but could not predict long-term survival in this study. So, SRSE may provide useful prognostic information for LV remodeling in patients in the early phase of an AMI.

REFERENCES

1. Hanekom L, Jenkins C, Jeffries L, Case C, Mundy J, Hawley C, et al. Incremental value of strain rate analysis as an adjunct to wall-motion scoring for assessment of myocardial viability by dobutamine echocardiography: a follow-up study after revascularization. Circulation 2005 Dec 20;112(25):3892-900.
2. Hoffmann R, Altiok E, Nowak B, Heussen N, Kühl H, Kaiser HJ, et al. Strain rate measurement by doppler echocardiography allows improved assessment of myocardial viability inpatients with depressed left ventricular function. Journal of the American College of Cardiology 2002;39(3):443-9.
3. Thibault H, Derumeaux G. Assessment of myocardial ischemia and viability using tissue Doppler and deformation imaging: the lessons from the experimental studies. Archives of cardiovascular diseases 2008;101(1):61-8.
4. Hoffmann R, Altiok E, Nowak B, Kühl H, Kaiser HJ, Buell U, et al. Strain rate analysis allows detection of differences in diastolic function between viable and nonviable myocardial segments. Journal of the American Society of Echocardiography 2005;18(4):330-5.
5. Eng C, Sonnenblick EH, Factor SM, Robinson TF, Zhang H, Zhao MJ. Profound structural alterations of the extracellular collagen matrix in postischemic dysfunctional ("stunned") but viable myocardium. Journal of the American College of Cardiology 1987;10(6):1322-34.
6. Cerisano G, Bolognese L, Carrabba N, Buonamici P, Santoro GM, Antoniucci D, et al. Doppler-derived mitral deceleration time: an early strong predictor of left ventricular remodeling after reperfused anterior acute myocardial infarction. Circulation 1999 Jan 19;99(2):230-6.
7. Rossi A, Cicoira M, Anselmi M, Golia G, Latina L, Tinto M, et al.

Myocardial viability independently influences left ventricular diastolic function in the early phase after acute myocardial infarction. J Am Soc Echocardiogr 2002 Dec;15(12):1490-5.

8. Bjork Ingul C, Rozis E, Slordahl SA, Marwick TH. Incremental value of strain rate imaging to wall motion analysis for prediction of outcome in patients undergoing dobutamine stress echocardiography. Circulation 2007 Mar 13;115(10):1252-9.
9. Mastouri R, Mahenthiran J, Kamalesh M, Gradus-Pizlo I, Feigenbaum H, Sawada SG. Prediction of ischemic events by anatomic M-mode strain rate stress echocardiography. J Am Soc Echocardiogr 2008 Apr;21(4):299-306.
10. Urheim S, Edvardsen T, Torp H, Angelsen B, Smiseth OA. Myocardial strain by Doppler echocardiography. Validation of a new method to quantify regional myocardial function. Circulation 2000 Sep 5;102(10):1158-64.
11. Abraham TP, Belohlavek M, Thomson HL, Pislaru C, Khandheria B, Seward JB, et al. Time to onset of regional relaxation: feasibility, variability and utility of a novel index of regional myocardial function by strain rate imaging. J Am Coll Cardiol 2002 May 1;39(9):1531-7.
12. Visser CA, Twisk J, Stoel MG, Kamp O, van der Heide JA, Mannaerts HF. Early identification of left ventricular remodelling after myocardial infarction, assessed by transthoracic 3D echocardiography. European Heart Journal 2004;25(8):680-7.
13. Antoniucci D, Santoro GM, Buonamici P, Cerisano G, Parodi G, Neskovic AN, et al. Left ventricular remodeling after primary coronary angioplasty: patterns of left ventricular dilation and long-term prognostic implications. Circulation 2002;106(18):2351-7.
14. Visser CA, Veen G, Verheugt FW, Kamp O, Nijland F. Long-term implications of reocclusion on left ventricular size and function after successful thrombolysis for first anterior myocardial infarction. Circulation 1997;95(1):111-7.

15. Bax J, Tanabe M, Chan Y, Schwartzman D, Fung JW, Suffoletto MS, et al. Usefulness of tissue Doppler velocity and strain dyssynchrony for predicting left ventricular reverse remodeling response after cardiac resynchronization therapy. The American journal of cardiology 2007;100(8):1263-70.
16. Len AR, Martin RP, Easley KA, Vera FV, DeLurgio DB, Smith AL, et al. Usefulness of the peak velocity difference by tissue Doppler imaging technique as an effective predictor of response to cardiac resynchronization therapy. The American journal of cardiology 2004;94(6):817-20.
17. Sanderson JE, Zhang Y, Kong S, Kum LC, Lin H, Chan Y, et al. Tissue Doppler imaging is superior to strain rate imaging and postsystolic shortening on the prediction of reverse remodeling in both ischemic and nonischemic heart failure after cardiac resynchronization therapy. Circulation 2004;110(1):66-73.
18. Edvardsen T, Gerber BL, Garot J, Bluemke DA, Lima JA, Smiseth OA. Quantitative assessment of intrinsic regional myocardial deformation by Doppler strain rate echocardiography in humans: validation against three-dimensional tagged magnetic resonance imaging. Circulation 2002 Jul 2;106(1):50-6.
19. Voigt JU, Exner B, Schmiedehausen K, Huchzermeyer C, Reulbach U, Nixdorff U, et al. Strain-rate imaging during dobutamine stress echocardiography provides objective evidence of inducible ischemia. Circulation 2003 Apr 29;107(16):2120-6.
20. Artis NJ, Oxborough DL, Williams G, Pepper CB, Tan LB. Two-dimensional strain imaging: a new echocardiographic advance with research and clinical applications. International journal of cardiology 2008;123(3):240-8.
21. Hanekom L, Cho GY, Leano R, Jeffriess L, Marwick TH. Comparison of two-dimensional speckle and tissue Doppler strain measurement during dobutamine stress echocardiography: an angiographic

correlation. European Heart Journal 2007;28(14):1765-72.
22. Wang J, Khoury DS, Thohan V, Torre-Amione G, Nagueh SF. Global diastolic strain rate for the assessment of left ventricular relaxation and filling pressures. Circulation 2007;115(11):1376-83.
23. Bree D, Wollmuth JR, Cupps BP, Krock MD, Howells A, Rogers J, et al. Low-dose dobutamine tissue-tagged magnetic resonance imaging with 3-dimensional strain analysis allows assessment of myocardial viability in patients with ischemic cardiomyopathy. Circulation 2006;114(1 Suppl):I33-6.

<ABSTRACT (IN KOREAN)>

급성 심근경색증 초기에 시행한 Strain Rate 스트레스 심초음파의 임상적 의의

<지도교수 정남식>

연세대학교 대학원 의학과

정 욱 진

Strain rate 스트레스 심초음파는 관동맥 질환이 의심되는 환자에서 고식적인 벽운동지수에 독립적이면서 부가적으로 예후를 나타냄이 보고되었다. 그렇지만, 급성심근경색증환자에서 strain rate 스트레스 심초음파가 좌심실 개조이나 예후에 어떠한 역할을 할 수 있는지는 알려진 바 없다. 또한 급성심근경색증에서 이완기나 시간 간격 strain rate 인자들에 대한 연구도 이루어진 바가 없었다. 따라서 본 연구에서는 급성심근경색증 초기에 저용량 도부타민 스트레스 심초음파를 이용한 strain rate 영상을 종합적으로 분석하여 초기 좌심실 이완 기능과 후기 좌심실 개조와의 연관성을 알아보고 더 나아가 예후 예측에 어떤 역할이 있는지를 알아보고자 하였다. 연속된 두 분절 이상에서 무운동을 보이는 급성

심근경색증 환자 134명에서 발병 5~9일째 저용량 도부타민 스트레스 심초음파를 시행하면서 기저 시와 도부타민 10μg/kg/min의 최대용량에서 조직도플러 영상을 각각 저장하였다. 저장된 영상에서 기저 시와 최대 용량 시에 각각, 최고 수축기 조직속도, 최고 수축기 strain 및 일곱가지의 strain rate 영상 지표들을 12 분절에서 측정하였고, 심근 경색이 온 분절들의 평균값, 그 평균값의 합 및 전체 분절의 평균값 들을 구하였다. 저용량 도부타민 스트레스 심초음파 6시간이내에 좌, 우 심도자 검사를 통해 좌심실 이완기압과 폐동맥 쐐기압을 측정하였다. 6개월후 추적 심초음파 검사와 NT-proBNP를 측정하였다. 연구 종료시 평균 50.0 ± 2.0개월간의 장기 추적 결과를 조사하였다. 최종적으로 45명의 환자(66.7% 남자, 평균 연령 58.6±1.9세, 66.7% 전벽 심근경색, 71.1% ST-분절 상승 심근경색)의 520 분절에서 분석이 이루어 졌다. 10mcg에서의 초기 충만기 strain rate의 전체 분절 평균값과 심방 수축기의 최고 strain rate에 이르는 시간의 전체 분절 평균값은 급성심근경색 초기의 E/E'비와 통계적으로 의미 있는 상관성을 보였다(r=-0.41 and p=0.02 and r=-0.35 and p=0.02). 심방 수축기의 최고 strain rate에 이르는 시간의 전체 분절 평균값과 초기 충만기 최고 strain rate에 이르는 시간의 경색 분절 평균값은 6개월후 좌심실 이완기 용적의 감소량이 20% 초과 증가하는 것으로 정의된 좌심실 개조를 독립적으로 예측할 수 있었다(β=-0.02 and p=0.04 and β=-0.04 and p=0.03). 장기간의 추적 관찰에서 사망을 예측할 수 있는 인자는 발견할 수 없었다. 이와 같은 결과에서 급성 심근경색증 초기에 저용량 도부타민을 투여하여

얻는 strain rate 스트레스 심초음파는 후기 좌심실 개조를 예측하는데 도움을 줄 수 있는 유용한 수단이라고 생각되며, 특히 이완기나 시간 간격 strain rate 인자들이 중요한 역할을 할 수 있을 것으로 사료된다.

핵심되는 말 : 심근 경색, 스트레스 심초음파, 도플러 심초음파, 좌심실 개조, 예후

PUBLICATION LIST

Chung WJ, Shin MS, Bong JM, Kang WC, Han SH, Moon CI, Koh KK, ahn TH, Chin IS, Shin EK. Effects of myocardial viability assessed by strain stress echocardiography on diastolic function in acute myocardial infarction. Circulation. 2008;118: S_655-6.